Bioorganic Chemistry 109 (2021) 104708

Contents lists available at ScienceDirect

Bioorganic Chemistry

journal homepage: www.elsevier.com/locate/bioorg

Telomerase activators from 20(27)-octanor-cycloastragenol via biotransformation by the fungal endophytes

Seda Duman [a], Güner Ekiz [b,c], Sinem Yılmaz [d,e], Hasan Yusufoglu [f], Petek Ballar Kırmızıbayrak [g], Erdal Bedir [a,*]

[a] Department of Bioengineering, Faculty of Engineering, İzmir Institute of Technology, 35430 Urla-İzmir, Turkey
[b] Department of Pharmaceutical Microbiology, Faculty of Pharmacy, Near East University, Nicosia, Mersin 10, Turkey
[c] Department of Bioengineering, Graduate School of Natural and Applied Sciences, Ege University, 35100 Bornova-İzmir, Turkey
[d] Department of Bioengineering, Faculty of Engineering, University of Alanya Aladdin Keykubat, Antalya 07400, Turkey
[e] Department of Biotechnology, Graduate School of Natural and Applied Sciences, Ege University, 35100 Bornova-İzmir, Turkey
[f] Department of Pharmacognosy, College of Pharmacy, Prince Sattam Bin Abdulaziz University, 11942 Al-Kharj, Saudi Arabia
[g] Department of Biochemistry, Faculty of Pharmacy, Ege University, 35100 Bornova-İzmir, Turkey

ARTICLE INFO

Keywords:
Saponins
Cycloastragenol
Endophytic fungi
Fungal biotransformation
Telomerase activation
Potent metabolites

ABSTRACT

Cycloastragenol [20(*R*),24(*S*)-epoxy-3β,6α,16β,25-tetrahydroxycycloartane] (CA), the principle sapogenol of many cycloartane-type glycosides found in *Astragalus* genus, is currently the only natural product in the anti-aging market as telomerase activator. Here, we report biotransformation of 20(27)-octanor-cycloastragenol (**1**), a thermal degradation product of CA, using *Astragalus* species originated endophytic fungi, viz. *Penicillium roseopurpureum*, *Alternaria eureka*, *Neosartorya hiratsukae* and *Camarosporium laburnicola*. Fifteen new biotransformation products (**2**–**16**) were isolated, and their structures were established by NMR and HRESIMS. Endophytic fungi were found to be capable of performing hydroxylation, oxidation, ring cleavage-methyl migration, dehydrogenation and Baeyer-Villiger type oxidation reactions on the starting compound (**1**), which would be difficult to achieve by conventional synthetic methods. In addition, the ability of the metabolites to increase telomerase activation in Hekn cells was evaluated, which showed from 1.08 to 12.4-fold activation compared to the control cells treated with DMSO. Among the compounds tested, **10**, **11** and **12** were found to be the most potent in terms of telomerase activation with 12.40-, 7.89- and 5.43-fold increase, respectively (at 0.1, 2 and 10 nM concentrations, respectively).

1. Introduction

Cycloartane-type saponins from *Astragalus* species and their semi-synthetic derivatives have been shown to exhibit a broad range of biological properties, including immunomodulatory, antineoplastic, antiprotozoal, and wound healing [1–3]. The most important and commercially significant development in *Astragalus* studies has been the discovery of cycloastragenol (CA), the main aglycone of *Astragalus* cycloartane-type glycosides, as a telomerase activator by the systematic screening of natural product extracts from traditional Chinese medicines in 2000 [4]. This compound was licensed and introduced into the food supplement market as an anti-aging product under the brand name TA-65 in 2007 [5].

Telomerase is a cellular reverse transcriptase (*TERT*, telomerase reverse transcriptase) that catalyzes the addition of TTAGGG repeats to the ends of telomers by using a corresponding RNA component (*Terc*, telomerase RNA component) [6]. Telomeres, the protective ends of chromosomes, shorten progressively with each cell division in the absence of telomerase enzyme. Telomere loss leads to critically shortened telomers that triggers replicative senescence, and it has been proposed as a major cause of aging and age-related diseases. In addition, mutations in the telomerase maintenance genes are associated with the development of certain diseases, including dyskeratosis congenita, pulmonary fibrosis, aplastic anemia, and liver fibrosis [6–8]. Thus, telomerase activators (TA) have been suggested as promising agents for healthy aging and in the treatment of telomere-driven diseases [9–11]. Due to their unique biological activity, viz. telomerase activation, the preparation of cycloastragenol analogs with improved anti-aging

* Corresponding author.
E-mail address: erdalbedir@iyte.edu.tr (E. Bedir).

https://doi.org/10.1016/j.bioorg.2021.104708
Received 7 October 2020; Received in revised form 24 December 2020; Accepted 28 January 2021
Available online 8 February 2021

activity has attracted increased attention recently.

Biotransformation is a powerful method for structure modification of complex molecules to generate a variety of derivatives and/or novel structures which is hard or almost impossible to produce through chemical synthesis [12–14]. Whole-cell catalysts provide a natural environment for the enzymes, allow transformation of organic compounds via multistep reactions with cofactor regeneration, and are more readily and inexpensively prepared catalyst formulations in comparison with the isolated enzymes [15–19]. Among microorganisms, filamentous fungi have been the most preferred whole-cell systems for the modification of triterpenoids [20,21]. Particularly, endophytic fungi have gained great attention as biocatalysts in biotransformation studies due to their ability to modify complex natural products such as steroids and triterpenoids with a high degree of stereospecificity [22–25].

Our previous studies revealed the promising potential of plant-associated endophytic fungi to transform plant-derived natural products [26,27]. In continuation of our research on the transformation of *Astragalus* cycloartanes, the present work reports the biotransformation of 20(27)-octanor-cycloastragenol (**1**), a thermal degradation product of cycloastragenol, using endophytic fungi obtained from *Astragalus* species. As a result, 15 new derivatives (**2**–**16**) of **1** were isolated through the preparative-scale studies. The effect of the biotransformation products in increasing telomerase activation in Hekn cells was evaluated using the *TeloTAGGG* telomerase PCR ELISA kit.

2. Results and discussion

The capability of 15 fungal endophytes, isolated from different parts of two *Astragalus* species (*A. angustifolius* and *A. condensatus*), to transform **1** into new metabolites was investigated. Based on the initial screening results, further studies were carried out using four fungi, viz. *Penicillium roseopurpureum*, *Alternaria eureka*, *Neosartorya hiratsukae*, and *Camarosporium laburnicola*. The preparative-scale biotransformation studies on **1** with the selected fungi generated fifteen metabolites (**2**–**16**) (Fig. 1), two from *P. roseopurpureum* (**2** and **3**), seven from *A. eureka* (**3**–**9**), two from *C. laburnicola* (**10** and **11**), and six from *N. hiratsukae* (**4** and **12**–**16**). The structures of **2**–**16** were established by analysis of NMR and HR-ESI-MS data.

The metabolite **2** gave a molecular formula of $C_{22}H_{32}O_3$ based on the HR-ESI-MS data (*m/z* = 345.2445, calcd. for $[M+H]^+$: 345.2429). The AX system signals of 9,19-cyclopropane ring and four methyl groups in the up-field region were observed unchanged when compared to **1**. The disappearance of low-field characteristic signals belonging to the H-3 and H-16 protons in the ^{1}H NMR spectrum and the appearance of two carbonyl carbons (δ_C = 216.8 and 218.7) in the ^{13}C NMR spectrum, suggested oxidation at C-3 and C-16 (Tables 1 and 3). The long-range correlations from H_3-28 and H_3-29 protons to the carbon at δ_C = 216.8, and from H-17 and H-15 resonances to δ_C = 218.7 supported the presence of the carbonyl groups at C-3 and C-16, respectively. Consequently, the structure of **2** was determined as 3,16-dioxo derivative of 20(27)-octanor-cycloastragenol (Yield: 1.43%).

The molecular formula of metabolite **3** was established as $C_{22}H_{31}O$ by HR-ESI-MS analysis (*m/z* = 311.2397, calcd. for $[M+H-2H_2O]^+$: 311.2375). The low-field signal of H-16 in **1** was absent in the ^{1}H-NMR spectrum, whereas a carbonyl signal at δ_C = 219.1 was observed in the ^{13}C NMR spectrum, suggesting oxidation at C-16. The HMBC correlations of H_2-15 and H_2-17 with the carbonyl carbon at δ_C = 219.1, verified the oxidation of OH-16. Thus, the structure of **3** was elucidated as 16-oxo derivative of 20(27)-octanor-cycloastragenol (Yield: 0.64%).

The metabolite **4** had a molecular formula of $C_{22}H_{36}O_4$ based on the HR-ESI-MS data (*m/z* = 387.2502, calcd. for $[M+Na]^+$: 387.2511). When compared to **1**, the absence of the characteristic cyclopropane ring signals in the ^{1}H NMR spectrum of **4** implied a ring cleavage. In the DEPT-135 and ^{13}C NMR spectra, the presence of a new oxymethylene resonance at δ_C = 68.9 in the low field suggested a monooxygenation, whereas two double bond signals (δ_C = 135.8 and 133.7) were also apparent in the carbon spectrum. In the HSQC spectrum, the double bond carbons did not show correlation to any proton, substantiating the presence of a tetrasubstituted olefinic system. Based on our previous studies with those of *Astragalus* sapogenols metabolized by *Cunninghamella blakesleeana* NRRL 1369 and *Alternaria eureka* 1E1BL1 [26,28,29], **4** was proposed to go through a ring-cleavage followed by a methyl migration affording a C-9(10) double bond with a primary alcohol substitution at C-11. This assumption was also confirmed with the $^2J_{H\text{-}C}$ and $^3J_{H\text{-}C}$ correlations in the HMBC spectrum from H-5 to C-10; H-1 to C-9/C-10, and H_2-12 to C-19 (Fig. 2). The methyl migration to position C-11 created a new stereocenter on the structure. Relative stereochemistry of this center was determined by evaluating the ROESY correlations. The δ_H = 4.03 resonance (one of the H_2-19 protons) in the low field showed strong correlation with the δ_H = 2.98 signal (one of the H-1 protons). This H-1 proton was not interacting with H-5 implying that it was on the upper face (β) of the molecule as drawn. On the other hand, the weak interaction of the other H-19 proton (δ_H = 3.90), with both H_3-18 and the δ_H = 2.47 signal of H-12, correlating with each other, substantiated that the C-19 had β configuration, which finalized the structure of **4** as shown in Fig. 1 (Yield: 0.22%).

In the HR-ESI-MS spectrum of **5**, a major ion peak was observed at *m/z* 395.1992 $[M+Cl]^-$ suggesting the molecular formula $C_{22}H_{32}O_4$ (calcd. for $[M+Cl]^-$: 395.1995). The ^{1}H NMR spectrum of **5** was very similar to that of **2**, except for the absence of one of the cyclopropane ring signals (δ_H = 0.61, H-19b) from the upfield region and the appearance of an oxymethine proton at δ_H = 4.31. A detailed inspection of the COSY and HSQC spectra revealed that H-19a (δ_H = 1.70) undergone a significant downfield shift (ca. 1.0 ppm) compared to **1**. The observed down-field shift is a common feature of C-11 hydroxylated cycloartanes [30]. The proton at δ_H = 4.31, which corresponded to a carbon at δ_C = 64.5 in the HSQC spectrum, was readily assigned to H-11 verifying monooxygenation. The ^{13}C NMR spectrum of **5** was low-quality due to its scarce amount; therefore, the carbon data was unambiguously determined by the HSQC and HMBC spectra. So, the carbonyl carbons resonating over 210 ppm verified the oxidations in the structure. Accordingly, the $^3J_{H\text{-}C}$ long-distance interactions of H_3-28 (δ_H = 1.50) and H_3-29 (δ_H = 1.80) protons with one of these carbonyl signals in the HMBC spectrum, and low-field shift of the H-2 proton signals (δ_H = 2.61 and 2.74) substantiated the oxidation at C-3. The proton signals originating from the methylene groups detected in the HSQC (H_2-15: δ_H = 2.12, 2.37; H_2-17: δ_H = 2.07, 2.47) resonated in the lower field slightly, whereas these protons showed cross peaks with the other carbonyl carbon in the HMBC spectrum. Based on this data, the second carbonyl group was undoubtedly located at C-16. In addition, the low-field shift of C-12 resonance together with the $^3J_{H\text{-}C}$ long-distance correlation of one of H_2-12 protons (δ_H = 2.55) with δ_C = 64.5 signal were evident to prove abovementioned hydroxylation at C-11. The orientation of C-11(OH) was determined by evaluating the ROESY spectrum. The interaction between H-11 (δ_H = 4.31) and H_3-30 (δ_H = 1.04) was evident to conclude that C-11(OH) was β-oriented. As a result, the structure of **5** was identified as 11(β)-hydroxy,3,16-dioxo-20(27)-octanor-cycloastragenol (Yield: 0.03%).

In the HR-ESI-MS of **6**, a major ion peak was observed at *m/z* 397.2149 indicating a molecular formula of $C_{22}H_{34}O_4$ (calcd. for $[M+Cl]^-$: 397.2151). In the ^{1}H NMR spectrum, the characteristic signals of 9,19-cyclopropane ring were lacking, which implied a ring cleavage as in **4**. The similarity between the spectral data of **4** and previously reported biotransformation products of cycloastragenol [28,31] not only supported our assumption but also enabled us to determine the relative stereochemistry of C-19 to be β. However, when **6** was compared to compound **4**, the low field characteristic signal of H-16 was absent in the ^{1}H NMR spectrum of **6**. In the HMBC spectrum, the $^3J_{H\text{-}C}$ long-distance correlations of H_2-15 (δ_H = 2.05 and 2.38) and H_2-17 (δ_H = 2.43 and 2.03) with the carbonyl carbon at δ_C = 211.1 suggested the oxidation at C-16. Consequently, it was established that compound **6** was 16-keto derivative of **4** (Fig. 1) (Yield: 0.04%).

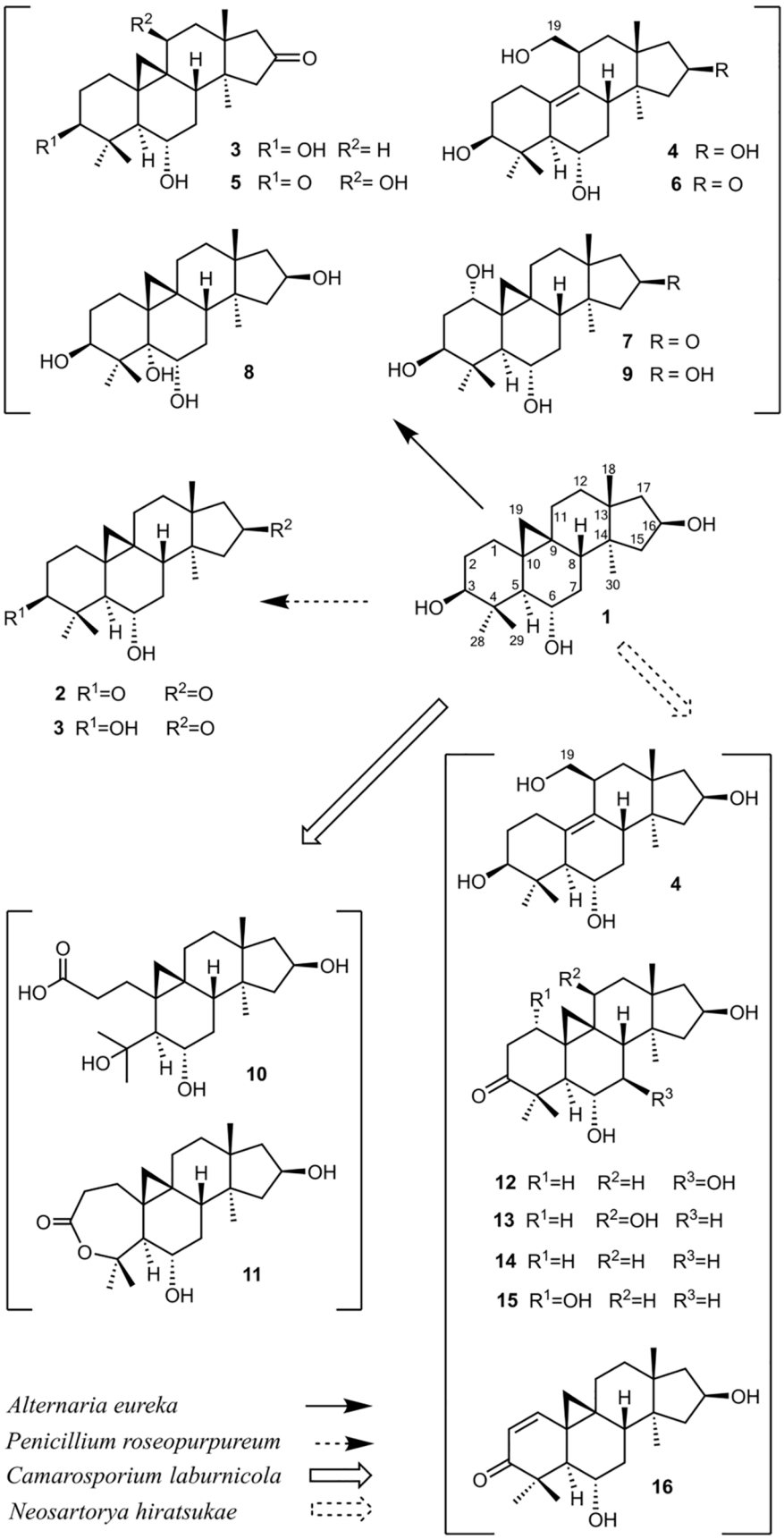

Fig. 1. Structures of **1** and its biotransformation products (**2**–**16**) by *Alternaria eureka*, *Penicillium roseopurpureum*, *Camarosporium laburnicola* and *Neosartorya hiratsukae*.

Table 1
^{1}H NMR data for compounds **1**–**8** (*J* in Hz, 500 MHz, in pyridine-d_5).

H	1	2[a]	3[a]	4	5	6	7	8
1	1.28 m, 1.66 m	1.26 m, 1.58 m	1.25 m, 1.57 m	2.98 d (10.5), 1.91 m	1.98 m, 2.38 m	2.95 d (11.9), 1.88 m	3.83 brs	1.85 m, 1.88 m
2	1.62 m, 1.74 m	1.61 m, 1.70 m	1.61 m, 1.71 m	1.91 m, 2.10 m	2.61 m, 2.74 ddd (13.4, 7.6, 5.6)	2.10 m, 1.90 m	2.30 m, 2.53 m	2.16 m, 2.08 m
3	3.23 dd (10.8, 4.6)	3.32 dd (10.9, 4.4)	3.22 dd (4.4, 10.9)	3.79 m		3.80 dd (10.5, 4.5)	4.54 dd (11.8, 4)	4.52 dd (11.4, 4.4)
4								
5	1.34 m	1.33 m	1.34 d (9.9)	2.34 d (6.8)	2.32 d (9.3)	2.34 d (6.6)	2.81 d (8.9)	
6	3.41 m	3.45 dt (9.8, 3.3)	3.44 m	4.20 m	3.87 m	4.18 m	3.99 m	4.08 t (8.6)
7	1.35 m, 1.41 m	1.38 m, 1.46 m	1.35 m, 1.41 m	1.83 m, 2.09 m	1.70 m, 1.81 m	1.94 m, 1.74 m	1.81 m, 1.85 m	1.51 m, 2.77 m
8	1.64 m	1.81 dd (12.1, 3.9)	1.78 m	2.41 d (11.5)	2.20 dd (11.5, 4.6)	2.54 m	1.99 m	1.77 m
9								
10								
11	1.75 dd (9.3, 13.3), 2.0 dd (13.3, 5.1)	1.19 m, 1.99 m	1.16 m, 2.09 m	3.42 m	4.31 m	3.39 m	2.54 m, 1.61 m	1.20 m, 2.23 m
12	3.82 dd (3.9, 5.9)	1.65 m (2H)	1.44 m, 2.11 m	1.96 dd (8.0, 13.8), 2.47 d (13.8)	1.98 m, 2.55 dd (14.2, 8.8)	2.53 d (14.1), 1.90 m	1.59 m, 1.91 m	1.72 m, 1.55 m
13								
14								
15	1.41 m, 2.02 m	1.43 m, 2.04 m	1.41 m, 2.15 dd (13.2, 8.5)	1.83 m, 2.14 m	2.12 d (17.7), 2.37 m	2.05 d (17.5), 2.38 d (17.5)	2.01 d (21), 1.98 m	1.82 m, 2.07 m
16	4.46 ddd (5.4, 7.9, 7.9)	4.46 ddd (5.6, 7.6, 7.6)	4.19 dd (5.8, 8.2)	4.86 m				4.81 dd (14.1, 7.0)
17	2.30 dd (11.0, 7.8)	2.08 m		2.05 m, 2.13 m	2.07 d (17.9), 2.47 d (18.1)	2.03 d (18), 2.43 d (18)	2.09 d (20.6), 2.06 (18.5)	2.06 m, 2.14 m
18	1.10 s	1.18 s	1.23 s	1.10 s	1.38 s	1.17 s	1.20 s	1.14 s
19	0.47 d, 0.50 d (4.5)	0.38 d (4.3), 0.53 d (4.1)	0.43 d (4.2), 0.51 d (4.2)	3.90 t (11.0), 4.03 m	0.61 d (4.3), 1.70 d (3.9)	4.02 dd (10.6, 5.1), 3.88 t (11.1)	0.37 d (4.1), 0.78 d (4.2)	0.55 d (4.3), 0.70 d (4.4)
28	1.24 s	1.22 s	1.24 s	1.83 s	1.50 s	1.83 s	1.94 s	1.52 s
29	0.95 s	0.95 s	0.96 s	1.13 s	1.80 s	1.12 s	1.40 s	1.93 s
30	1.02 s	0.99 s	1.28 s	1.23 s	1.04 s	0.86 s	1.25 s	1.33 s

[a] The data were recorded at 400 MHz in $CDCl_3$.

Table 2
^{1}H NMR data for compounds **9**–**16** (*J* in Hz, 500 MHz, in pyridine-d_5).

H	9	10[b]	11[b]	12	13	14	15	16
1	3.80 brs	1.74 m, 2.73 m	1.29 td (5.6, 13.6), 1.28 dd (5.9, 12.0)	2.04 m, 1.35 m	2.45 m, 2.04 m	1.31 m, 2.03 m	4.02 brs	6.85 d (10)
2	2.27 td (12.9, 2.8), 2.45 m	3.04 m, 2.73 m	2.91 td (13.3, 7.2), 2.62 dd (13.3, 4.5)	2.53 ddd (13.9, 6.9, 1.5)	2.74 m, 2.60 m	2.75 m, 2.47 m	2.90 dd (14.5, 3.2), 3.13 d (4.3)	6.23 d (10)
3	4.50 dd (12.0, 4.4)							
4								
5	2.79 d (9.4)	2.40 d (8.1)	2.41 d (9.4)	1.91 d (10.0)	2.33 d (9.5)	2.23 d (9.6)	3.16 dd (7.2, 2.5)	2.55 d (9.4)
6	3.96 m	4.11 m	3.67 td (10.4, 2.8)	3.76 t (9.4)	3.88 brs	3.73 t (9.0)	3.93 d (3.2)	3.96 dd (9.8, 5.3)
7	1.86 m, 1.88 m	1.86 m, 1.66 m	1.55 m, 1.70 m	3.63 t (7.3)	1.87 m, 1.87 m	1.66 m, 1.81 m	1.86 m, 1.88 m	1.75 m, 2.09 m
8	1.53 m	1.43 d (12.4)	1.48 m	2.39 d (12.8)	2.03 m	1.70 m	1.81 m	2.12 m
9								
10								
11	1.53 d (9.8), 2.65 t (10.3)	2.45 m, 1.24 dd (14, 10.7)	0.84 dd (14.4, 10.7), 2.10 m	2.08 m	4.37 t, (5.7)	1.07 m, 2.08 m	1.47 m, 2.70 m	1.76 m, 1.41 m
12	1.89 m, 2H	1.55 m, 1.74 m	1.51 m, 1.72 m	1.55 m, 1.77 m	2.60 m, 1.90 m	1.52 m, 1.74 m	1.55 m, 1.82 m	1.76 m, 2.14 m
13								
14								
15	1.82 m, 2.07 m	1.85 m, 2.03 m	1.83 d (13.3), 2.04 m	2.14 m	2.11 m, 1.86 m	2.10 m,	1.83 m, 2.09 m	1.76 m, 2.07 m
16	4.81 q (7.3)	4.81 dd (7.3, 7.4)	4.82 dd (14.8, 7.4)	4.87 dd (14.8, 7.9)	4.84 q (7.6)	4.82 dd (7.7, 14.9)	4.82 dd (7.2, 14.6)	4.83 q (6.5)
17	2.02 m, 2.06 m	2.10 m, 2.03 m	2.04 m, 2.09 m	2.64 dd (14.4,8.6), 2.72 tdd (7.7, 4.8, 1.89)	2.09 m, 2.07 m	1.83 m, 2.07 m	2.03 dd (12.7, 6.3), 2.10 dd (7.75, 12.6)	2.07 m, 2H
18	1.13 s	1.14 s	1.10 s	1.19 s	1.25 s	1.12 s	1.15 s	1.04 s
19	0.40 d (4.4), 0.75 d (4.3)	1.09 d (4.2), 0.61 d (4.2)	0.52 d (4.7), 0.76 d (4.7)	0.84 d (4.3), 0.36 d (4.3)	0.56 d (4.4), 1.76 d (4.3)	0.33 d (4.2), 0.68 d (4.2)	0.56 d (4.4), 0.87 d (4.4)	0.06 d (4.4), 1.22 d (4.4)
28	1.96 s	1.81 s	1.94 s	1.77 s	1.82 s	1.78 s	1.93 s	1.87 s
29	1.41 s	1.66 s	1.70 s	1.44 s	1.52 s	1.47 s	1.46 s	1.28 s
30	1.48 s	1.37 s	1.34 s	1.56 s	1.34 s	1.36 s	1.38 s	1.44 s

[b] The data were recorded at 400 MHz in pyridine-d_5.

Table 3
^{13}C NMR data for compounds **1**–**16** (125 MHz, pyridine-d_5).

C	1	2[a]	3[a]	4	5	6	7	8	9	10[b]	11[b]	12[b]	13	14	15	16
1	33.1	31.7	31.8	29.9	30.6	29.4	73.0	27.8	73.0	32.8	33.0	32.3	30.3	32.4	72.9	154.3
2	31.9	35.7	30.3	33.8	37.1	33.4	39.4	31.2	39.4	33.1	34.3	36.5	37.0	36.4	46.7	127.4
3	78.8	216.8	78.4	78.1	214.6	77.7	74.1	73.3	74.0	176.8	174.4	216.9	217.9	217.2	215.8	205.3
4	42.9	50.3	41.6	43.0	51.3	42.9	43.1	44.7	43.0	76.4	86.1	50.9	51.2	51.0	51.2	47.9
5	53.5	53.5	53.5	58.3	54.7	57.9	47.1	76.5	47.3	54.0	53.9	54.4	55.0	54.0	47.7	51.3
6	68.3	69.2	68.1	68.4	68.4	67.8	68.2	70.3	69.0	71.8	71.7	75.1	69.0	69.5	68.9	65.7
7	39.1	37.7	37.7	38.4	39.0	38.0	38.6	32.3	39.4	38.0	38.3	73.7	39.6	39.0	39.3	36.7
8	47.0	46.3	44.7	41.8	46.5	40.1	45.4	47.5	47.6	47.6	48.8	51.8	48.3	48.4	48.0	43.9
9	21.6	21.2	21.1	133.7	29.3	136.0	22.2	33.6	22.1	25.7	22.1	20.8	29.4	27.0	23.0	31.5
10	30.0	28.6	29.1	135.8	29.9	138.1	34.2	46.4	34.4	29.6	26.6	27.8	28.8	29.0	34.6	25.7
11	27.1	25.7	25.8	40.2	64.5	39.3	26.1	26.6	26.5	27.4	27.2	27.3	64.8	21.4	26.4	27.7
12	31.7	30.0	29.8	32.1	44.8	30.9	31.1	30.8	30.5	31.8	31.5	31.4	46.1	31.5	31.3	31.3
13	46.9	41.2	41.4	46.6	42.3	44.2	42.3	46.1	45.5	45.0	45.0	45.8	45.9	46.8	45.2	45.6
14	45.5	43.9	44.0	45.6	44.7	41.4	45.0	44.7	46.9	47.1	46.7	46.7	46.1	45.4	46.6	47.2
15	48.6	50.9	50.5	47.3	51.1	49.6	52.2	48.4	49.0	49.9	49.6	49.9	48.7	50.3	48.9	47.6
16	71.6	218.7	219.1	71.7	212.4	211.1	211.0	70.9	71.6	71.8	71.6	71.8	71.7	71.6	71.3	71.3
17	50.2	51.8	51.8	50.0	52.3	52.1	51.2	49.5	50.2	50.5	50.4	51.5	50.2	49.1	50.0	49.7
18	25.9	25.4	24.8	24.8	25.8	23.9	25.3	25.7	26.1	27.4	27.1	26.4	26.3	21.7	26.2	24.7
19	30.2	30.8	29.4	68.9	22.1	68.2	29.5	34.2	31.8	33.7	32.4	31.1	22.4	31.2	30.5	28.5
28	29.7	27.7	27.9	27.9	21.3	27.6	29.6	17.1	29.8	34.1	32.1	28.4	28.8	28.9	27.3	25.8
29	16.6	20.3	15.3	15.8	28.7	15.5	16.0	24.1	15.9	29.3	28.6	20.9	21.3	21.0	21.8	21.2
30	21.1	19.8	19.5	20.7	21.2	19.3	19.9	20.7	21.0	21.7	21.7	20.8	22.6	26.5	20.9	20.3

[a] The data were recorded at 100 MHz in $CDCl_3$. [b]The data were recorded at 100 MHz in pyridine-d_5.

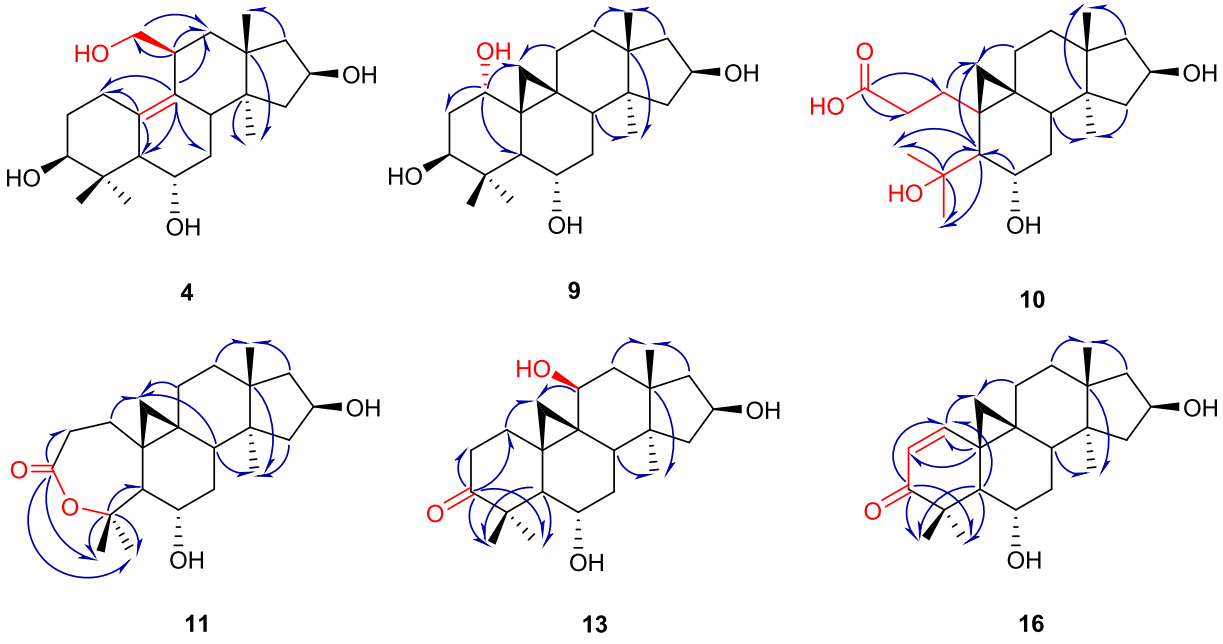

Fig. 2. Key HMBC's of compounds **4**, **9**–**11**, **13** and **16**.

In the HR-ESI-MS spectrum of **7**, a major ion peak was observed at *m/z* 399.2273 (calcd. for $[M+K-2H]^-$: 399.1943) indicating a molecular formula of $C_{22}H_{34}O_4$. The low-field signal of H-16 was not present in the ^{1}H NMR spectrum. A broad singlet proton was observed at 3.83 ppm, suggesting a transformation via monooxygenation. In the ^{13}C NMR spectrum, a new resonance at δ_C = 211.0 was observed, implying the oxidation of C-16(OH). The proton and carbon resonances assigned to the D ring for **7** were compatible with **2**, **3**, **5** and **6** indicating their similarity. The cross peaks between H_2-15 (δ_H = 2.01 and 1.98)/H_2-17 (δ_H = 2.09 and 2.06) and the new carbonyl signal in the HMBC spectrum, verified the carbonyl position to be C-16. By the HSQC spectrum, the corresponding carbon signal of the new proton at δ_H = 3.83 was determined to be δ_C = 73.0. In the COSY spectrum, the δ_H = 3.83 proton coupled with a methylene group (H_2-2; δ_H = 2.30 and 2.53), which, in turn, showed correlations with the characteristic signal of H-3 (δ_H = 4.54, dd, J = 11.8, 4.0 Hz) helping us to locate the hydroxylation at C-1. As a matter of fact, in the HMBC spectrum, the $^3J_{H\text{-}C}$ long-distance correlations between H_2-19 protons and δ_C = 73.0 confirmed the assumption. The orientation of C-1(OH) was found to be α based on the ROESY cross peak between H-1 and β-oriented H-19a at δ_H = 0.37. Thus, the structure of **7** was established as 1(α)-hydroxy,16-oxo derivative of 20,27-octanor cycloastragenol (Yield: 0.13%).

The HR-ESI-MS data of **8** (*m/z* 387.2499, calcd. for $[M+Na]^+$: 387.2511, $C_{22}H_{36}O_4Na$), displayed 16 amu increase over **1**, implying a monohydroxy derivative. The signals of 9,19-cycloprapane ring and four methyl groups, and H-3, H-6 and H-16 resonances were readily apparent in the ^{1}H NMR spectrum. A new oxygenated carbon signal at δ_C = 76.5 was present in the ^{13}C NMR spectrum substantiating the hydroxylation deduced based on the HR-ESI-MS data. In the HSQC spectrum, no correlation of this carbon with any proton suggested a tertiary alcohol

group. This carbon resonance was unambiguously assigned to C-5 based on the long-distance $^{3}J_{H\text{-}C}$ correlations in the HMBC spectrum from H_3-28 and H_3-29 protons to $\delta_C = 76.5$. The COSY spectrum also helped us to locate the exchangeable protons of C-3(OH) and C-6(OH) due to the $^{3}J_{H\text{-}H}$ couplings with H-3 and H-6 protons. The other exchangeable proton resonating at δ_H 4.25 (s) was assigned to C-5(O*H*), which showed a cross peak with H_3-28 (δ_H 1.52) in the ROESY spectrum, suggesting their co-facial orientation. Thus, C-5(OH) was located on the alpha face of **8**. Consequently, the structure of **8** was established as 5(α)-hydroxy derivative of 20(27)-octanor-cycloastragenol (Yield: 0.07%).

In the HR-ESI-MS spectrum of **9**, a major ion peak was observed at *m/z* 403.2440 (calcd. for $[M+K]^+$: 403.2246) revealing not only the molecular formula of $C_{22}H_{36}O_4$, but also another monooxygenated metabolite due to 16 amu difference compared to the substrate (**1**). Examination of the ^{1}H NMR spectrum revealed a broad singlet signal at 3.80 ppm, which agreed with hydroxyl group insertion as in compound **7**. Additionally, the observed correlation in the HMBC spectrum (Fig. 2) were confirmed the location of hydroxyl group at C-1. The relative stereochemistry at C-1 was determined by the ROESY spectrum. The orientation of C-1(OH) was deduced to be α on the basis of a cross peak between equatorially localized H-1 signal and H-19b at 0.40 ppm. Thus, the structure of **9** was established as 1(α)-hydroxy derivative of 20(27)-octanor-cycloastragenol (Yield: 0.04%).

In the HR-ESI-MS spectra of **10**, the molecular ion peaks were observed at *m/z* 403.2443 (calcd. for $[M+Na]^+$: 403.2455) suggesting a molecular formula of $C_{22}H_{36}O_5$. The 1D NMR spectra of **10** were similar to those of the starting compound except for the signals corresponding to the A ring. Major differences between **10** and **1** in the ^{13}C NMR spectrum were the absence of C-3 oxymethine signal and the additional resonances belonging to a carboxyl carbon ($\delta_C = 176.8$) and an oxygenated tertiary carbon at $\delta_C = 76.4$. As no significant alteration was observed on the spectral data of B, C and D rings, a modification on the A ring was suggested. The HMBC correlation of H-5, H_3-28 and H_3-29 protons to carbon at $\delta_C = 76.4$ verified the hydroxylation at C-4 (Fig. 2). The fact that the carboxyl carbon at 176.8 ppm did not interact with CH_3-28/ CH_3-29 while interacting with two methylene groups proposed that **10** went through a cleavage reaction in the A-ring via Baeyer–Villiger type oxidation followed by hydrolysis. The observed data was consistent with those of 3,4-seco cycloartane metabolites, which were established during biotransformation studies with the fungus *Glomerella fusarioides* earlier [29,31]. Since our spectral data were completely parallel with the previously determined biotransformation products, the structure of **10** was established unambiguously (Yield: 10%).

The molecular formula of **11** was established as $C_{22}H_{34}O_4$ based on its HR-ESI-MS data (*m/z* = 385.2369, calcd. for $[M+Na]^+$: 385.2354). Comparison of the NMR data of **11** with those of **1** suggested another A-ring modified analog. In the HMBC spectrum, the methylene protons (H_2-1 and H_2-2) and H_3-28/ H_3-29 displayed correlations with the carboxyl carbon at $\delta_C = 174.4$. Two methyl groups ($\delta_H = 1.94$ and 1.70; respectively CH_3-28 and CH_3-29) showed HMBC correlations with the tertiary carbon at 86.1 ppm, implying that it was C-4 (Fig. 2). The downfield shift of C-4 resonance (ca. 10 ppm) compared to **10** and spectral data comparison with similar metabolites reported previously [29] revealed that the A ring was transformed into a 7-membered lactone ring as a result of the catalysis of Baeyer-Villiger-type P450 monooxygenase enzyme. Thus, the structure of **11** was established as 3 (4)-olide derivative of **1** (Yield: 28%).

The molecular formula of **12** was determined to be $C_{22}H_{34}O_4$ on the basis of its HR-APCI-MS data (*m/z* = 363.2537, calcd. for $[M+H]^+$: 363.2535). The disappearance of low-field H-3 signal in the ^{1}H NMR spectrum as well as appearance of a carbonyl resonance at δ 216.9 in the ^{13}C NMR spectrum indicated oxidation of the secondary alcohol at C-3. Moreover, a new proton signal observed at $\delta_H = 3.63$ (t, $J = 7.3$ Hz), which was correlating with a carbon at $\delta_C = 73.7$ in the HSQC, implied a transformation via monooxygenation. In the COSY spectrum, the $\delta_H = 3.63$ proton coupled with $\delta_H = 3.76$ (H-6, t, $J = 9.4$ Hz) and $\delta_H = 2.39$ (H-8), helping us to locate the hydroxyl group at C-7. The long-range HMBC correlations from H-5, H-6 and H-8 to C-7 also verified the proposed transformation. The orientation of C-7(OH) was found to be β based on the NOESY cross-peak between H-7 and α-oriented H-5. Thus, the structure of **12** was established as 7(β)-hydroxy,3-oxo derivative of 20,27-octanor cycloastragenol (Yield: 0.25%).

The HR-ESI-MS spectrum of **13** indicated a molecular formula of $C_{22}H_{34}O_4$ (*m/z* = 385.2347, calcd. for $[M+Na]^+$: 385.2354). Initial inspection of the ^{1}H NMR spectrum of **13** displayed that one of the distinctive 9,19-cyclopropane ring signals was missing. Examination of the COSY and HSQC spectra revealed that H_2-19 protons were resonating at $\delta_H = 1.76$ and 0.56, suggesting hydroxylation at C-11 as in **5**. A new signal observed at 4.37 ppm (t, $J = 5.7$ Hz), corresponded to a carbon at $\delta_C = 64.8$ in the HSQC spectrum, was readily assigned to H-11. On the other hand, loss of the characteristic H-3 signal with an additional carbonyl carbon at $\delta_C = 217.9$ in the ^{13}C NMR spectrum suggested oxidation of OH-3. In the HMBC spectrum, the key long-range correlations from H_3-28 and H_3-29 to C-3, and from H-19a and H-12b to C-11 verified the abovementioned transformations (Fig. 2). The orientation of C-11(OH) was proposed to be β based on the spectral data comparison with those of **5**. Thus, the structure of **13** was established as 11(β)-hydroxy,3-oxo derivative of 20,27-octanor cycloastragenol (Yield: 0.16%).

In the HR-ESI-MS spectrum of **14**, a major ion peak was observed at *m/z* 369.2385 $[M+Na]^+$ suggesting a molecular formula of $C_{22}H_{34}O_3$ (calcd. for $[M+Na]^+$: 369.2400). Its 1D NMR spectra were closely related to those of the starting compound (**1**). The distinct differences between **14** and **1** were that the characteristic H-3 signal was lost in the ^{1}H NMR spectrum, and a new carbonyl resonance ($\delta_C = 217.2$) was observed instead of the corresponding oxymethine carbon in the ^{13}C NMR spectrum of **14**. This carbonyl carbon at $\delta_C = 217.2$ was readily assigned to C-3 based on its HMBC correlations with H_3-28 ($\delta_H = 1.78$)/ H_3-29 ($\delta_H = 1.47$) and H-5 ($\delta_C = 2.23$, d, $J = 9.6$ Hz). Thus, the structure of **14** was established as 3-oxo derivative of 20,27-octanor cycloastragenol (Yield: 0.13%).

In the HR-ESI-MS spectrum of **15**, a quasimolecular ion peak was observed at *m/z* 385.2345 proposing a molecular formula of $C_{22}H_{34}O_4$ (calcd. for $[M+Na]^+$: 385.2349). 1D NMR spectra of **15** were very similar to those of **14**, except for the additional signals corresponding to an oxygen bearing methine group ($\delta_H = 4.02$ brs; δ_C 72.9). The carbonyl signal observed at $\delta_C = 215.8$ was assigned to C-3 due to its HMBC correlations with H_3-28 ($\delta_H = 1.93$)/H_3-29 ($\delta_H = 1.46$) and H-5 ($\delta_H = 3.16$, dd, $J = 7.2$, 2.5 Hz). The new hydroxy group was located at C-1 on the basis of the COSY correlation of H-1 ($\delta_H = 4.02$) with H-2a ($\delta_H = 3.13$, d, $J = 4.3$ Hz), and the long-distance correlation between the 72.9 ppm carbon signal and H_2-19 ($\delta_H = 0.56$, d, $J = 4.4$ Hz; $\delta_H = 0.87$, d, $J = 4.4$ Hz)/H-5 ($\delta_H = 3.16$, dd, $J = 7.2$, 2.5 Hz). The relative stereochemistry at C-1 was deduced based on the NOESY spectrum. H-1 ($\delta_H = 4.02$ brs) showed correlation with one of the H_2-19 protons ($\delta_H = 0.56$, d, $J = 4.4$ Hz), which provided evidence for the α-orientation of the hydroxy group at C-1. Accordingly, metabolite **15** was assigned as 1(α)-hydroxy,3-oxo derivative of 20(27)-octanor-cycloastragenol (Yield: 0.06%).

The molecular formula of **16** was established as $C_{22}H_{32}O_3$ by HR-ESI-MS (*m/z* 367.2236, calcd. for $[M+Na]^+$: 367.2244), indicating seven degrees of unsaturation. The main differences between **16** and **1** were that one of the distinctive cyclopropane ring signals and H-3 resonance were missing in the ^{1}H NMR spectrum, and two additional protons of a disubstituted double bond were present ($\delta_H = 6.85$, d, $J = 10.0$ Hz; $\delta_H = 6.23$, d, $J = 10.0$ Hz). Accordingly, two olefinic carbon resonances ($\delta_C = 154.3$ and 127.4) were observed in the ^{13}C NMR spectrum of **16** together with a carbonyl resonance at δ_C 205.3, which were substantiating additional two degrees of unsaturation and oxidation at C-3. The cross peaks between the carbonyl signal in the HMBC spectrum and H_3-28 (1.87, s)/H_3-29 (1.28, s)/H-5 (2.55, d, $J = 9.4$ Hz), and the low-field olefinic proton (6.85, d, $J = 10$ Hz) not only verified the oxidation at C-3 but also located the double bond between C-1 and C-2 (Fig. 2).

Additionally, the long-range correlations from H_2-19/H-5 to the signal at δ_C = 154.3 (C-1) confirmed the proposed structure. Consequently, metabolite **16** was deduced to be 3-oxo,1(2)-ene derivative of 20(27)-octanor-cycloastragenol (Yield: 0.03%).

The biotransformation products with sufficient amount were tested on telomerase activation by PCR-based ELISA assay. Based on the preliminary work [27], the selected metabolites were screened in different concentration ranges of 0.1–30 nM; 0.5–30 nM or 30–1000 nM. Cycloastragenol (CA) was used as an experimental positive control. Telomerase enzyme activation by the compounds ranged from 1.08 to 12.4-fold compared to the control cells treated with DMSO (Table S1, Supporting Information). Among the compounds, **10** and **11** were found to be the most potent telomerase activators. Specifically, metabolite **11** with 7-membered lactone ring provided telomerase activation of 7.89- and 6.19-fold at 2 and 10 nM concentrations, respectively. Compound **10**, a further metabolite of **11**, found to be the most potent compound at the lowest test dose (12.4-fold activation at 0.1 nM) in our screening studies.

From biotransformation point of view, the endophytic fungus *P. roseopurpureum* could catalyse oxidation reactions at C-3 and C-16 positions to produce 3,16-oxo (**2**) and 16-oxo (**3**) derivatives. *A. eureka* was found to be capable of monooxygenation, oxidation and ring cleavage-methyl migration transformations on the substrate as parallel to our previous reports [26,27]. The monooxygenation reactions occurred at positions C-1 (**7** and **9**), C-5 (**8**) and C-11 (**5**), whereas the oxidation reactions afforded C-3 and/or C-16 oxo products (**3**–**7**). The cleavage of 9,19-cyclopropane ring followed by migration of C-19 from C-10 to C-11 position as well as monooxygenation of C-19 to the primary alcohol (**4**) were notable. This unique reaction was first revealed by our group in the biotransformation study of cycloastragenol and *C. blakesleeana* NRRL 1369, forming a new triterpene skeleton [28]. The same enzymatic reaction was also observed for **6** together with an additional modification at C-16 as oxidation. *N. hiratsukae* mainly catalyzed monooxygenation and oxidation reactions as reported previously [26]. This fungus oxidized the secondary alcohol at C-3 regioselectively to give 3-oxo derivatives of **1**, whereas monooxygenation reactions provided C-1 (**15**), C-7 (**12**) and C-11 (**13**) hydroxylated metabolites. Apart from the aforementioned reactions, *N. hiratsukae* led to methyl migration (**4**) and Δ^1-dehydrogenation (**16**) reactions on **1**. In the case of *C. laburnicola*, the Baeyer-Villiger oxidation reaction was predominant to give A-ring modified metabolites. Specifically, lactone formation in **11** catalyzed by the Baeyer-Villiger monooxygenase (BVMO). After lactone ring formation, a hydrolase enzyme catalyzes a further step to yield 3,4-seco metabolites. Subsequently, C-3 is transformed to a carboxylic acid, whereas C-4/C-28/C-29 isopropyl cation forms, which undergoes a nucleophilic attack by H_2O to afford a tertiary alcohol at C-5 (**10**). This cascade reaction of *C. laburnicola* was also observed previously [27] implying the importance of the newly discovered fungus [32] as a whole-cell system specifically for BVMO initiated ring cleavage.

From chemistry point of view, as expected, the C-1 and C-11 positions were more susceptible to the monooxygenation due to the presence of cyclopropane ring giving allylic character to these methylene carbons. On the other hand, another active but sterically hindered C-5 position was subject to hydroxylation. A monooxygenation at C-5 position has been encountered for the first time in triterpenoid biotransformation studies. Moreover, the presence of a hydroxy group at C-7 position has been rarely reported in triterpene chemistry. In *Astragalus* cycloartanes, C-7 hydroxylated secondary metabolites have only been reported from *Astragalus oleifolius* [33,34]; however, C-6/C-7 diol system is found as a unique feature of **12**.

In conclusion, biotransformation of 20(27)-octanor-cycloastragenol (**1**) with the endophytic fungi afforded fifteen new metabolites (**2**–**16**). Hydroxylation, oxidation, ring cleavage-methyl migration, dehydrogenation and Baeyer-Villiger type oxidation reactions were observed on the steroid nucleus, which would be difficult to achieve by traditional synthetic methods. This study, together with our previous reports [26,27], revealed that biotransformation using plant-associated fungal endophytes is a powerful tool to generate structural diversity in compound libraries. In addition, we speculate that A-ring modification, viz. **10** and **11,** is important to obtain potent activators of telomerase. However, further studies are warranted to establish structure-activity relationships confidently by preparing and testing new analogs of 20 (27)-octanor-cycloastragenol and cycloastragenol towards telomerase activation and to elucidate mechanism of action at molecular level.

3. Experimental section

3.1. General experimental procedures

The substrate (purity > 98%), 20(27)-octanor-cycloastragenol, was donated by Bionorm Natural Products (İzmir, Turkey). Mass spectra were recorded on an Agilent 1200/6530 Instrument-HRTOFMS. The NMR spectra were obtained on Varian Oxford AS400 and Bruker DRX-500 instruments. FT-IR spectra were recorded using a Perkin Elmer Spectrum Two UATR-IR spectrometer. Column chromatography was performed using Silica gel 60 (70–230 mesh, Merck), Sephadex LH-20 (GE Healthcare Life Sciences) and RP-18 (Chromabond C18, Macherey-Nagel). Silica gel 60 F254 (Merck) and RP-18 F254s (Merck) plates were used for thin layer chromatography (TLC) analyses. Spots were visualized under UV light and by spraying with 20% aqueous H_2SO_4 solution followed heating.

3.2. Fungal strains

A total of 15 endophytic fungi were isolated from various tissues of *Astragalus* plants, as described previously [26]. *Alternaria eureka* 1E1BL1 and *Camarosporium laburnicola* 1E4BL1 were characterized by the Identification Service of the DSMZ (Braunschweig, Germany) using ITS, LSU and TEF1 sequence data [35,36]. *Neosartorya hiratsukae* 1E2AR1-1 and *Penicillium roseopurpureum* 1E4BS1 were also identified by ITS analysis. The original cultures were deposited at the Bedir Laboratory with the deposit numbers 20131E1BL1, 20131E4BL1, 20131E2AR1-1, and 20131E4BS1 [37]. The strains were maintained on potato dextrose agar (PDA) slants and stored at 4 °C.

3.3. Biotransformation procedures

The analytical and preparative scale studies were carried out as described previously [31]. The following liquid media were used: Medium I (2% glucose, 0.5% yeast extract, 0.5% NaCl, 0.5% K_2HPO_4 and 0.5% peptone (w/v), pH 6.0) and Medium II (potato-dextrose broth = PDB). Analytical scale studies were conducted using 250 mL flasks containing 50 mL of liquid medium. The substrate (**1**) was added to each flask as a solution in DMSO (10 mg dissolved in 500 µl), and the flasks were then incubated at 25 °C and 180 rpm. The samples (1 mL) were taken every other day for 21 days and centrifuged. The supernatants were then extracted with an equal volume of EtOAc and analyzed by TLC. Control flasks were also incubated in the absence of either **1** or the fungus. In preparative scale, 1000 mL Erlenmeyer flasks containing 300 mL of medium and 60 mg of substrate were used at the same conditions as analytical scale. The preparative scale experiments were conducted using 1600 mg of **1** with *P. roseopurpureum* for 12 days in Medium I, 2000 mg of **1** with *A. eureka* (in Medium I) and 4000 mg of **1** with *A. eureka* (in Medium II) for 14 days, 500 mg of **1** with *C. laburnicola* for 6 days in Medium II, and 4000 mg of **1** with *N. hiratsukae* in Medium II for 18 days (25 °C and 180 rpm). After the incubation period, the cultures were filtered, and the combined filtrate was extracted with an equal volume of EtOAc. The organic phase was dried over anhydrous Na_2SO_4, and the solvent was removed under reduced pressure at 40 °C to yield the crude extracts.

3.4. Isolation of the transformation products

Penicillium roseopurpureum: The EtOAc extract (2 g) was chromatographed on a silica gel column (150 g) eluted with cyclohexane-EtOAc (1:1, *v/v*) and cyclohexane-EtOAc-MeOH (10:10:0.5 to 10:10:1, *v/v*) gradient, to afford 10.6 mg **2** and four subfractions (A-D). Subfraction B (34 mg) was subjected to vacuum liquid chromatography (VLC) on reversed-phase material (RP-18, 20 g), using MeOH-H_2O gradient (65:35 to 100:0, *v/v*) to give **1** (23 mg).

***Alternaria eureka* (in Medium I)**: Compounds **4**–**7** were obtained from the EtOAc extract (2.4 g) of *A. alternata* with **1**. This crude extract was first subjected to a Sephadex LH-20 (75 g) column, using MeOH as eluent, to provide one main fraction (1.5 g). This fraction was then subjected to VLC on reversed-phase silica gel (RP-18, 40 g), using an ACN-H_2O gradient (15:85 to 100:0, *v/v*), yielding three main fractions (A-C). Fraction A (31 mg) was chromatographed on a silica gel column (10 g) eluted with $CHCl_3$-MeOH (95:5, *v/v*) to afford metabolite **4** (4.3 mg). Fraction B (33 mg) was subjected to a silica gel column (10 g) with the solvent system $CHCl_3$-MeOH (98:2 to 96:4, *v/v*) to give three subfractions. Subfraction 1 was then applied to VLC using reversed-phase material (RP-18, 10 g), eluting with MeOH- H_2O (75:25) to give 0.7 mg of **6**. Fraction C (23 mg) was further fractionated over silica gel column (10 g) eluted with $CHCl_3$-MeOH (98:2 to 96:4, *v/v*) to give **7** (2.5 mg) and fraction C1 (5.2 mg). To purify metabolite **5** (0.5 mg), fraction C1 was applied to VLC (RP-18, 10 g) and eluted with MeOH-H_2O (45:55, *v/v*).

***Alternaria eureka* (in Medium II)**: The EtOAc extract (4.46 g) was first chromatographed on a Sephadex LH-20 (75 g) column and eluted with MeOH-$CHCl_3$ (1:1), which provided 70 fractions. Fractions 21 to 27 were pooled (785.5 mg) and subjected to separation on a silica gel column (200 g) using *n*-hexane-EtOAc-MeOH (10:10:1 to 10:10:2, *v/v*), yielding seven fractions (A-G). Fraction A (46.2 mg) was applied to VLC (RP-C18, 25 g), eluting with ACN-H_2O (25:75 to 30:70, *v/v*) and MeOH, to give **3** (6.2 mg) and five fractions (A1-5). To isolate metabolite **8** (2.9 mg), fraction D (109.8 mg) was submitted to silica gel column (70 g), using CH_2Cl_2-MeOH (98:2 to 92:8, *v/v*). Fraction F (16.5 mg) was further fractionated over a silica gel column (15 g) and eluted with CH_2Cl_2-MeOH (92:8, *v/v*), to afford five fractions (F1-5). Fraction F5 (5.7 mg) was purified by silica gel column chromatography (15 g), with the solvent system CH_2Cl_2-MeOH (95:5 to 90:10, *v/v*), to provide **7** (0.8 mg). Fraction G (89.8 mg) was subjected to VLC (RP-C18, 30 g), using ACN-H_2O gradient (15:85 to 100:0 *v/v*), yielding five fractions (G1-5). To purify metabolite **9** (1.6 mg), fraction G5 (9.4 mg) was subjected to a silica gel column chromatography (15 g) and eluted with CH_2Cl_2-MeOH (90:10, *v/v*).

Camarosporium laburnicola: The EtOAc extract (652 mg) was first subjected to VLC (RP-18, 40 g), eluting with ACN-H_2O (30:70, *v/v*), to afford 140 mg of **11** and fraction 4–12. Fraction 4–12 was evaporated in vacuo until only water remains. The H_2O phase was transferred into a separatory funnel and the pH value was adjusted to 12 by adding ammonia and shaken with an equal volume of $CHCl_3$. Following the phase separation, the aqueous phase was collected, and the pH was adjusted to 4 by adding formic acid. The partition step was repeated with $CHCl_3$. Finally, $CHCl_3$ phases containing **10** (50 mg) were collected and evaporated to dryness.

Neosartorya hiratsukae: The crude extract (6.982 g) was subjected to Sephadex LH-20 column chromatography (90 g), eluting with EtOAc-MeOH (1:1, *v/v*) and MeOH, which provided 75 fractions. Fractions 20 to 46 were pooled (2.55 g) and subjected to a silica gel column (165 g) to yield four main fractions (A-D). Fraction A was submitted to silica gel column (40 g) using $CHCl_3$-MeOH (100:0 to 0:100, *v/v*) to give three fractions ($A_{1\text{-}3}$). Fraction A_2 (33.9 mg) was further applied on VLC (RP-18, 35 g) and eluted with MeOH-H_2O (60:40, *v/v*) to afford fraction A_2-1 (48.2 mg). To purify metabolite **13** (6.2 mg), fraction A_2-1 was subjected to silica gel column (80 g) with the solvent system *n*-hexane-EtOAc-MeOH (10:10:0.5, *v/v*). Fraction C (60.7 mg) was applied to a Sephadex LH-20 column (30 g) and eluted with MeOH, which provided fraction C_1 (45.2 mg). This fraction was applied to VLC (RP-C18, 35 g) using ACN-H_2O (35:65, *v/v*) to afford two fractions (C_1-1 and C_1-2). Fraction C_1-1 (11.2 mg) was separated on VLC (RP-C18, 10 g) with the solvent system ACN-H_2O (15:85 to 25:75, *v/v*) to give fraction C_1-1a (7.1 mg). This fraction was then purified on silica gel column (13 g) using $CHCl_3$-EtOH (97.5:2.5 to 0:100, *v/v*) to give 2.3 mg of **15**. Fraction C_1-2 (15.3 mg) was chromatographed over a silica gel column (15 g), with the solvent system $CHCl_3$-MeOH (100:0 to 95:5, *v/v*), yielding fraction C_1-2a (6.3 mg). This fraction was then applied to VLC (RP-C18, 10 g) and eluted with ACN-H_2O (30:70 to 60:40, *v/v*) to give 55 fractions. Fraction 38 to 50 were combined (3 mg) and further purified on a silica gel column (8 g) using $CHCl_3$- EtOH (100:0 to 97.5:2.5, *v/v*) to afford **16** (1 mg). Fraction B (396 mg) was chromatographed on VLC using reversed-phase material (RP-C18, 40 g), eluting with ACN-H_2O (25:75 to 60:40, *v/v*) and MeOH, yielding three fractions ($B_{1\text{-}3}$). Fraction B_1 (22.4 mg) was further fractionated on a silica gel column (14 g) and eluted with *n*-hexane-EtOAc-MeOH (10:10:1, *v/v*) to provide fraction B_1-1 (8.2 mg). This fraction was then subjected to VLC (RP-C18, 10 g) with the solvent system ACN-H_2O (30:70, *v/v*) to give 10 fractions. Fractions 6 and 7 were pooled (7.9 mg) and further purified by VLC (RP-C18, 10 g) with the solvent system ACN-H_2O (15:85 to 25:75, *v/v*) to give 10.1 mg of **12**. Fraction B_2 (10.2 mg) was also applied on VLC (RP-C18, 10 g) using ACN-H_2O (20:80 to 25:75, *v/v*) and MeOH to yield metabolite **14** (5 mg) and fraction B_2-1 (1.8 mg). Fraction B_3 (62.1 mg) was fractionated with Sephadex LH-20 column chromatography (30 g) and eluted with MeOH to give fraction B_3-1 (15.2 mg). Fraction D (44 mg) was also chromatographed on a Sephadex LH-20 column (30 g), eluting with MeOH, which provided 45 fractions. Fractions 21 to 24 were pooled for further purification. This fraction (12.6 mg) and fraction B_3-1 (15.2 mg) were combined and applied to VLC (RP-C18, 35 g) and eluted with MeOH-H_2O (30:70, *v/v*) to give 50 fractions. Fraction 22 to 34 were then pooled together for further purification. This fraction (4.2 mg) and fraction B_2-1 (1.8 mg) were combined and submitted to a silica gel column (15 g) with the solvent system $CHCl_3$-MeOH (95:5 to 85:15, *v/v*) to give 80 fractions. In order to isolate metabolite **4** (0.9 mg), fractions 69 to 75 were pooled and further purified by VLC (RP-C18, 10 g) using ACN-H_2O (30:70 to 60:40, *v/v*).

3.5. Structural characterization

Compound 2: (2aR,5aS,5bS,7S,7aR,11aR,12aS)-7-hydroxy-2a,5a,8,8-tetramethyldodecahydro-4H,12H-cyclopenta[*a*]cyclopropa[e]phenanthrene-4,9(5H)-dione; 1.43% yield; $[\alpha]^{29}_{D}$ −30 (*c* 0.53, MeOH); IRυ_{max} 3402, 2948, 2836, 1735, 1413, 1386, 1027, 755 cm^{-1}; HR-ESI-MS: *m/z* = 345.2445, calcd. for $[M+H]^+$: 345.2429, corresponding to $C_{22}H_{32}O_3$; ^1H NMR (400 MHz, $CDCl_3$) and ^{13}C NMR (100 MHz, $CDCl_3$), data, see Tables 1 and 3.

Compound 3: (2aR,5aS,5bS,7S,7aR,9S,11aR,12aS)-7,9-dihydroxy-2a,5a,8,8-tetramethyltetradecahydro-4H,12H-cyclopenta[*a*]cyclopropa[e]phenanthren-4-one; 0.64% yield; $[\alpha]^{29}_{D}$ −47 (*c* 0.17, MeOH); IRυ_{max} 3376, 2946, 2832, 1732, 1660, 1452, 1415, 1120, 1025, 755, 667 cm^{-1}; HR-ESI-MS: *m/z* = 311.2397, calcd. for $[M+H\text{-}2H_2O]^+$: 311.2375, corresponding to $C_{22}H_{34}O_3$; ^1H NMR (400 MHz, $CDCl_3$) and ^{13}C NMR (100 MHz, $CDCl_3$), data, see Tables 1 and 3.

Compound 4: (3S,5R,6S,8S,11S,13R,14S,16R)-11-(hydroxymethyl)-4,4,13,14-tetramethyl-2,3,4,5,6,7,8,11,12,13,14,15,16,17-tetradecahydro-1H-cyclopenta[*a*]phenanthrene-3,6,16-triol; 0.22% yield; $[\alpha]^{29}_{D}$ −27 (*c* 0.15, MeOH); IRυ_{max} 3364, 2948, 2834, 1453, 1419, 1126, 1024, 755, 667 cm^{-1}; HR-ESI-MS: *m/z* = 387.2502, calcd. for $[M+Na]^+$: 387.2511, corresponding to $C_{22}H_{36}O_4$; ^1H NMR (500 MHz, pyridine-d_5) and ^{13}C NMR (125 MHz, pyridine-d_5), data , see Tables 1 and 3.

Compound 5: (1S,2aR,5aS,5bS,7S,7aR,11aR,12aR)-1,7-dihydroxy-2a,5a,8,8-tetramethyldodecahydro-4H,12H-cyclopenta[*a*]cyclopropa[e]phenanthrene-4,9(5H)-dione; 0.03% yield; $[\alpha]^{29}_{D}$ −100 (*c* 0.02,

MeOH); IRυ_{max} 3358, 2948, 2834, 1453, 1417, 1124, 1025, 755, 665 cm^{-1}; HR-ESI-MS: m/z = 395.1992, calcd. for $[M+Cl]^-$: 395.1995, corresponding to $C_{22}H_{32}O_4$; ^1H NMR (500 MHz, pyridine-d_5) and ^{13}C NMR (125 MHz, pyridine-d_5), data, see Tables 1 and 3.

Compound 6: (3S,5R,6S,8S,11S,13R,14S)-3,6-dihydroxy-11-(hydroxymethyl)-4,4,13,14-tetramethyl-1,2,3,4,5,6,7,8,11,12,13,14,15,17-tetradecahydro-16H-cyclopenta[*a*]phenanthren-16-one; 0.04% yield; $[\alpha]^{29}_D$ −200 (*c* 0.02, MeOH); IRυ_{max} 3365, 2947, 2834, 1452, 1414, 1022, 755, 667 cm^{-1}; HR-ESI-MS: m/z = 397.2149, calcd. for $[M+Cl]^-$: 397.2151, corresponding to $C_{22}H_{34}O_4$; ^1H NMR (500 MHz, pyridine-d_5) and ^{13}C NMR (125 MHz, pyridine-d_5), data, see Tables 1 and 3.

Compound 7: (2aR,5aS,5bS,7S,7aS,9S,11S,11aS,12aS)-7,9,11-trihydroxy-2a,5a,8,8-tetramethyltetradecahydro-4H,12H-cyclopenta[*a*]cyclopropa[e]phenanthren-4-one; 0.13% yield; $[\alpha]^{29}_D$ −25 (*c* 0.08, MeOH); IRυ_{max} 3379, 3269, 3015, 2947, 2834, 1418, 1125, 1026, 756, 667 cm^{-1}; HR-ESI-MS: m/z = 399.2273, calcd. for $[M+K-2H]^-$: 399.1943, corresponding to $C_{22}H_{34}O_4$; ^1H NMR (500 MHz, pyridine-d_5) and ^{13}C NMR (125 MHz, pyridine-d_5), data, see Tables 1 and 3.

Compound 8: (2aR,4R,5aS,5bS,7S,7aS,9S,11aS,12aS)-2a,5a,8,8-tetramethyltetradecahydro-7aH,12H-cyclopenta[*a*]cyclopropa[e]phenanthrene-4,7,7a,9-tetraol; 0.07% yield; IRυ_{max} 3357, 2948, 2835, 1660, 1451, 1418, 1221, 1122, 1025, 755, 667 cm^{-1}; HR-ESI-MS: m/z = 387.2499, calcd. for $[M+Na]^+$: 387.2511, corresponding to $C_{22}H_{36}O_4$; ^1H NMR (500 MHz, pyridine-d_5) and ^{13}C NMR (125 MHz, pyridine-d_5), data, see Tables 1 and 3.

Compound 9: (2aR,4R,5aS,5bS,7S,7aS,9S,11S,11aS,12aS)-2a,5a,8,8-tetramethyltetradecahydro-1H,12H-cyclopenta[*a*]cyclopropa[e]phenanthrene-4,7,9,11-tetraol; 0.04% yield; IRυ_{max} 3362, 2947, 2835, 1665, 1452, 1413, 1125, 1025, 755, 667 cm^{-1}; HR-ESI-MS: m/z = 403.2440, calcd. for $[M+K]^+$: 403.2246, corresponding to $C_{22}H_{36}O_4$; ^1H NMR (500 MHz, pyridine-d_5) and ^{13}C NMR (125 MHz, pyridine-d_5), data, see Tables 2 and 3.

Compound 10: 3-((2R,3aS,3bS,5S,6S,6aR,7aS,9aR)-2,5-dihydroxy-6-(2-hydroxypropan-2-yl)-3a,9a-dimethyldecahydro-1H-cyclopenta[*a*]cyclopropa[e]naphthalen-6a(7H)-yl)propanoic acid; 10% yield; $[\alpha]^{29}_D$ + 36 (*c* 0.11, MeOH); IRυ_{max} 3352, 3279, 3003, 2948, 2883, 1657, 1451, 1422, 1122, 1025, 755, 666 cm^{-1}; HR-ESI-MS: m/z = 403.2443, calcd. for $[M+Na]^+$: 403.2455, corresponding to $C_{22}H_{36}O_5$; ^1H NMR (400 MHz, pyridine-d_5) and ^{13}C NMR (100 MHz, pyridine-d_5), data, see Tables 2 and 3.

Compound 11: (5aR,6aS,8aR,10R,11aS,11bS,13S,13aS)-10,13-dihydroxy-1,1,8a,11a-tetramethyltetradecahydro-3H,6H-cyclopenta[5,6]cyclopropa[1,8a]naphtho[2,1-c]oxepin-3-one; 28% yield; $[\alpha]^{29}_D$ + 48 (*c* 0.21, MeOH); IRυ_{max} 3370, 3272, 2987, 2948, 2909, 2835, 1708, 1451, 1414, 1130, 1025, 755, 667 cm^{-1}; HR-ESI-MS: m/z = 385.2369, calcd. for $[M+Na]^+$: 385.2354, corresponding to $C_{22}H_{34}O_4$; ^1H NMR (400 MHz, pyridine-d_5) and ^{13}C NMR (100 MHz, pyridine-d_5), data, see Tables 2 and 3.

Compound 12: (2aR,4R,5aS,5bS,6R,7R,7aR,11aR,12aS)-4,6,7-trihydroxy-2a,5a,8,8-tetramethyltetradecahydro-9H,12H-cyclopenta[*a*]cyclopropa[e]phenanthren-9-one; 0.25% yield; IRυ_{max} 3370, 3282, 3002, 2946, 2907, 2833, 1664, 1417, 1219, 1125, 1025, 754, 665 cm^{-1}; APCI-ESI-MS: m/z = 363.2537, calcd. for $[M+H]^+$: 363.2535, corresponding to $C_{22}H_{34}O_4$; ^1H NMR (400 MHz, pyridine-d_5) and ^{13}C NMR (100 MHz, pyridine-d_5), data, see Tables 2 and 3.

Compound 13: (1S,2aS,4R,5aS,5bS,7S,7aR,11aR,12aR)-1,4,7-trihydroxy-2a,5a,8,8-tetramethyltetradecahydro-9H,12H-cyclopenta[*a*]cyclopropa[e]phenanthren-9-one; 0.16% yield; IRυ_{max} 3368, 3277, 2947, 2915, 2835, 1663, 1557, 1477, 1453, 1415, 1120, 1023, 756, 622 cm^{-1}; HR-ESI-MS: m/z = 385.2347, calcd. for $[M+Na]^+$: 385.2354, corresponding to $C_{22}H_{34}O_4$; ^1H NMR (500 MHz, pyridine-d_5) and ^{13}C NMR (125 MHz, pyridine-d_5), data, see Tables 2 and 3.

Compound 14: (2aR,4R,5aS,5bS,7S,7aR,11aR,12aS)-4,7-dihydroxy-2a,5a,8,8-tetramethyltetradecahydro-9H,12H-cyclopenta[*a*]cyclopropa[e]phenanthren-9-one; 0.13% yield; $[\alpha]^{27}_D$ + 90 (*c* 1.04, MeOH); IRυ_{max} 3362, 2947, 2976, 2832, 1700, 1449, 1219, 1116, 1025, 753, 665 cm^{-1}; HR-ESI-MS: m/z = 369.2385, calcd. for $[M+Na]^+$: 369.2400, corresponding to $C_{22}H_{34}O_3$; ^1H NMR (500 MHz, pyridine-d_5) and ^{13}C NMR (125 MHz, pyridine-d_5), data, see Tables 2 and 3.

Compound 15: (2aR,4R,5aS,5bS,7S,7aR,11S,11aS,12aS)-4,7,11-trihydroxy-2a,5a,8,8-tetramethyltetradecahydro-9H,12H-cyclopenta[*a*]cyclopropa[e]phenanthren-9-one; 0.06% yield; $[\alpha]^{28}_D$ + 40 (*c* 0.1, MeOH); IRυ_{max} 3352, 2945, 2832, 1652, 1449, 1415, 1219, 1116, 1023, 753, 666 cm^{-1}; HR-ESI-MS: m/z = 385.2345, calcd. for $[M+Na]^+$: 385.2349, corresponding to $C_{22}H_{34}O_4$; ^1H NMR (500 MHz, pyridine-d_5) and ^{13}C NMR (125 MHz, pyridine-d_5), data, see Tables 2 and 3.

Compound 16: (2aR,4R,5aS,5bS,7S,7aR,11aS,12aS)-4,7-dihydroxy-2a,5a,8,8-tetramethyl-1,2,2a,3,4,5,5a,5b,6,7,7a,8-dodecahydro-9H,12H-cyclopenta[*a*]cyclopropa[e]phenanthren-9-one; 0.03% yield; $[\alpha]^{28}_D$ −33 (*c* 0.06, MeOH); IRυ_{max} 3348, 2948, 2833, 1657, 1449, 1415, 1116, 1022, 753, 665 cm^{-1}; HR-ESI-MS: m/z = 367.2236, calcd. for $[M+Na]^+$: 367.2236, corresponding to $C_{22}H_{34}O_4$; ^1H NMR (500 MHz, pyridine-d_5) and ^{13}C NMR (125 MHz, pyridine-d_5), data, see Tables 2 and 3.

3.6. Biological activity assay

Cell Line and Culture Condition: Neonatal human primary epidermal keratinocytes (Hekn) considered in the literature as cells with low telomerase enzyme activity, were used in the screening of telomerase activation, which were obtained from American Type Culture Collection (ATCC; PCS-200-010) and cultured according to the manufacturer's protocol.

Telomerase Enzyme Activity Assay: Telomerase activity assays were done in Hekn cells of 4–6 days' PD (population doubling) time *via* PCR-based ELISA assay. In briefly, the experiment was carried out as follows. After seeding Hekn cells; the medium was refreshed on the following day. The day after, cells were treated with the desired doses of the test compounds for 24 h. After completion of the incubation period, cells were harvested, and $2x10^5$ cells were transferred to a new and prechilled Eppendorf tube. Then, cells were centrifuged and lysated in lysis buffer. The lysates were obtained after centrifugation at 16,000*g* for 20 min. Telomerase enzyme activity assay was performed via Telomerase PCR ELISA kit (Sigma-Aldrich, St. Louis, MO, USA) according to the manufacturer's instruction. The absorbances of negative/positive controls and samples were measured at a wavelength of 450 nm with a reference wavelength of approximately 690 nm by ELISA plate reader (Varioskan, Thermo Fisher Scientific, US).

Declaration of Competing Interest

The authors declare that they have no known competing financial interests or personal relationships that could have appeared to influence the work reported in this paper.

Acknowledgements

This project was supported by The Scientific and Technological Research Council of Turkey (TUBITAK, Project No: 114Z958). We are very grateful to Bionorm Natural Products for donating the substrate, and special thanks are due to the NMR spectrometer operator, Anzarulhaque Anwarulhaque, of Prince Sattam bin Abdulaziz University, Al-Kharj, Saudi Arabia.

Appendix A. Supplementary material

Supplementary data to this article can be found online at https://doi.org/10.1016/j.bioorg.2021.104708.

References

[1] E. Yesilada, E. Bedir, İ. Çalış, Y. Takaishi, Y. Ohmoto, Effects of triterpene saponins from *Astragalus* species on in vitro cytokine release, J. Ethnopharmacol. 96 (2005) 71–77.

[2] D. Gülcemal, O. Alankuş-Çalişkan, A. Perrone, F. Özgökçe, S. Piacente, E. Bedir, Cycloartane glycosides from *Astragalus aureus*, Phytochemistry 72 (2011) 761–768.

[3] A. Nalbantsoy, T. Nesil, S. Erden, İ. Çalış, E. Bedir, Adjuvant effects of *Astragalus* saponins Macrophyllosaponin B and Astragaloside VII, J. Ethnopharmacol. 134 (2011) 897–903.

[4] C. Harley, S. Khor, M. Ramaseshan, P. Ramiya, Z. Pirot, S. Fauce, T. Lin, Composition and Methods for Increasing Telomerase Activity (2010).

[5] C.B. Harley, W. Liu, M. Blasco, E. Vera, W.H. Andrews, L.A. Briggs, J.M. Raffaele, A natural product telomerase activator as part of a health maintenance program, Rejuvenation Res. 14 (2011) 45–56.

[6] B.B. de Jesus, K. Schneeberger, E. Vera, A. Tejera, C.B. Harley, M.A. Blasco, The telomerase activator TA-65 elongates short telomeres and increase health span of adult/old mice withhout increasing cancer incidence, Aging Cell 10 (2011) 604–621.

[7] P. Martínez, M.A. Blasco, Telomere-driven diseases and telomere-targeting therapies, J. Cell Biol. 216 (2017) 875–887.

[8] P.L. Opresko, J.W. Shay, Telomere-associated aging disorders, Ageing Res. Rev. 33 (2017) 52–66.

[9] P.-K. Ma, B.-H. Wei, Y.-L. Cao, Q. Miao, N. Chen, C.-E. Guo, H.-Y. Chen, Y.-J. Zhang, Pharmacokinetics, metabolism, and excretion of cycloastragenol, a potent telomerase activator in rats, Xenobiotica 47 (2017) 526–537.

[10] D. Tsoukalas, P. Fragkiadaki, A.O. Docea, A.K. Alegakis, E. Sarandi, M. Thanasoula, D.A. Spandidos, A. Tsatsakis, M.P. Razgonova, D. Calina, Discovery of potent telomerase activators: Unfolding new therape, Mol. Med. Rep. 20 (2019) 3701–3708.

[11] S.R. Fauce, B.D. Jamieson, A.C. Chin, R.T. Mitsuyasu, S.T. Parish, H.L. Ng, C.M. R. Kitchen, O.O. Yang, C.B. Harley, R.B. Effros, Telomerase-based pharmacologic enhancement of antiviral function of human $CD8^{+}$ T lymphocytes[1], J. Immunol. 181 (2008) 7400–7406.

[12] K.B. Borges, W.d.S. Borges, R. Durán-Patrón, M. T. Pupo, P.S. Bonato, I.G. Collado, Stereoselective biotransformations using fungi as biocatalysts, Tetrahedron: Asymmetry 20 (2009) 385–397.

[13] J. Tao, J.H. Xu, Biocatalysis in development of green pharmaceutical processes, Curr. Opin. Chem. Biol. 13 (2009) 43–50.

[14] R.N. Patel, Microbial/enzymatic synthesis of chiral intermediates for pharmaceuticals, Enzyme Microb. Technol. 31 (2002) 804–826.

[15] J.D. Carballeira, M.A. Quezada, P. Hoyos, Y. Simeó, M.J. Hernaiz, A.R. Alcantara, J.V. Sinisterra, Microbial cells as catalysts for stereoselective red-ox reactions, Biotechnol. Adv. 27 (2009) 686–714.

[16] T. Ishige, K. Honda, S. Shimizu, Whole organism biocatalysis, Curr. Opin. Chem. Biol. 9 (2005) 174–180.

[17] M. Schrewe, M.K. Julsing, B. Bu, A. Schmid, Whole-cell biocatalysis for selective and productive C-O functional group introduction and modification, Chem. Soc. Rev. 42 (2013) 6346–6377.

[18] C.C.C.R. de Carvalho, Whole cell biocatalysts: essential workers from Nature to the industry, Microb. Biotechnol. 10 (2017) 250–263.

[19] B. Lin, Y. Tao, Whole-cell biocatalysts by design, Microb. Cell Fact. 16 (2017) 106.

[20] S.A.A. Shah, H.L. Tan, S. Sultan, M.A.B.M. Faridz, M.A.B.M. Shah, S. Nurfazilah, M. Hussain, Microbial-catalyzed biotransformation of multifunctional triterpenoids derived from phytonutrients, Int. J. Mol. Sci. 15 (2014) 12027–12060.

[21] K. Muffler, D. Leipold, M.C. Scheller, C. Haas, J. Steingroewer, T. Bley, H. E. Neuhaus, M.A. Mirata, J. Schrader, R. Ulber, Biotransformation of triterpenes, Process Biochem. 46 (2011) 1–15.

[22] L.F. Bianchini, M.F.C. Arruda, S.R. Vieira, P.M.S. Campelo, A.M.T. Gregio, E.A. R. Rosa, Microbial biotransformation to obtain new antifungals, Front. Microbiol. 6 (2015) 1433.

[23] Y. Wang, C.C. Dai, Endophytes: a potential resource for biosynthesis, biotransformation, and biodegradation, Ann. Microbiol. 61 (2011) 207–215.

[24] W.D.S. Borges, K.B. Borges, P.S. Bonato, S. Said, M.T. Pupo, Endophytic fungi: natural products, enzymes and biotranformation reactions, Curr. Org. Chem. 13 (2009) 1137–1163.

[25] M.R. Pimentel, G. Molina, A.P. Dionísio, M.R. Maróstica Junior, G.M. Pastore, The use of endophytes to obtain bioactive compounds and their application in biotransformation process, Biotechnol. Res. Int. 2011 (2011).

[26] G. Ekiz, S. Duman, E. Bedir, Biotransformation of cyclocanthogenol by the endophytic fungus *Alternaria eureka* 1E1BL1, Phytochemistry 151 (2018) 91–98.

[27] G. Ekiz, S. Yılmaz, H. Yusufoglu, P.B. Kırmızıbayrak, E. Bedir, Microabial transformation of cycloastragenol and astragenol by Endophytic Fungi isolated from *Astragalus* species, J. Nat. Prod. 82 (2019) 2979–2985.

[28] M. Kuban, G. Öngen, E. Bedir, Biotransformation of cycloastragenol by *Cunninghamella blakesleeana* NRRL 1369 resulting in a novel framework, Org. Lett. 12 (2010) 4252–4255.

[29] E. Bedir, C. Kula, Ö. Öner, M. Altaş, Ö. Tağ, G. Öngen, Microbial transformation of *Astragalus* sapogenins using *Cunninghamella blaskesleeana* NRRL 1369 and *Glomerella fusarioides* ATCC 9552, J. Mol. Catal. B Enzym. 115 (2015) 29–34.

[30] S. Kadota, J.X. Li, K. Tanaka, T. Namba, Constituents of cimicifugae rhizoma II. Isolation and structures of new cycloartenol triterpenoids and related compounds from Cimicifuga foetida L, Tetrahedron 51 (1995) 1143–1166.

[31] M. Kuban, G. Öngen, I.A. Khan, E. Bedir, Microbial transformation of cycloastragenol, Phytochemistry 88 (2013) 99–104.

[32] S. Tibpromma, et al., Fungal diversity notes 491–602: taxonomic and phylogenetic contributions to fungal taxa, Fungal Diversity 83 (2017) 1–261.

[33] I. Çaliş, M. Zor, I. Saracoğlu, A. Işimer, H. Rüegger, Four novel cycloartane glycosides from *Astragalus oleifolius*, J. Nat. Prod. 59 (1996) 1019–1023.

[34] E. Bedir, I. Calis, I.A. Khan, Macrophyllosaponin E: a novel compound from the roots of *Astragalus oleifolius*, Chem. Pharm. Bull. 48 (2000) 1081–1083.

[35] C.L. Schoch, K.A. Seifert, S. Huhndorf, V. Robert, J.L. Spouge, C.A. Levesque, W. Chen, et al., Nuclear ribosomal internal transcribed spacer (ITS) region as a universal DNA barcode marker for Fungi, Proc. Natl. Acad. Sci. 109 (2012) 6241–6246.

[36] J.H.C. Woudenberg, J.Z. Groenewald, M. Binder, P.W. Crous, *Alternaria* redefined, Stud. Mycol. 75 (2013) 171–212.

[37] G. Ekiz, Research on Bioactive Secondary Metabolite Profile of *Septofusidium berolinense* and Biotransformation of Cycloartane Type Saponins by Endophytic Fungi, Department of Bioengineering. Ege University, İzmir, 2016.